$Ca_v3.2$ T-type calcium channel is required for the NFAT-dependent Sox9 expression in tracheal cartilage

Shin-Shiou Lin[a,b], Bing-Hsiean Tzeng[b,c], Kuan-Rong Lee[a], Richard J. H. Smith[d], Kevin P. Campbell[e,f], and Chien-Chang Chen[b,1]

[a]Institute of Molecular Medicine, National Tsing Hua University, Hsinchu 30013, Taiwan; [b]Institute of Biomedical Sciences, Academia Sinica, Taipei 11529, Taiwan; [c]Division of Cardiovascular Medicine, Department of Internal Medicine, Tri-Service General Hospital, National Defense Medical Center, Taipei 11490, Taiwan; and [d]Departments of Otolaryngology, Internal Medicine, Pediatrics, and Molecular Physiology and Biophysics, [e]Howard Hughes Medical Institute, and [f]Departments of Molecular Physiology and Biophysics, Neurology, and Internal Medicine, University of Iowa, Iowa City, IA 52242

Edited by Jason R. Rock, University of California, San Francisco, CA, and accepted by the Editorial Board April 10, 2014 (received for review December 12, 2013)

Intracellular Ca^{2+} transient is crucial in initiating the differentiation of mesenchymal cells into chondrocytes, but whether voltage-gated Ca^{2+} channels are involved remains uncertain. Here, we show that the T-type voltage-gated Ca^{2+} channel $Ca_v3.2$ is essential for tracheal chondrogenesis. Mice lacking this channel ($Ca_v3.2^{-/-}$) show congenital tracheal stenosis because of incomplete formation of cartilaginous tracheal support. Conversely, $Ca_v3.2$ overexpression in ATDC5 cells enhances chondrogenesis, which could be blunted by both blocking T-type Ca^{2+} channels and inhibiting calcineurin and suggests that $Ca_v3.2$ is responsible for Ca^{2+} influx during chondrogenesis. Finally, the expression of sex determination region of Y chromosome (SRY)-related high-mobility group-Box gene 9 (Sox9), one of the earliest markers of committed chondrogenic cells, is reduced in $Ca_v3.2^{-/-}$ tracheas. Mechanistically, Ca^{2+} influx via $Ca_v3.2$ activates the calcineurin/nuclear factor of the activated T-cell (NFAT) signaling pathway, and a previously unidentified NFAT binding site is identified within the mouse Sox9 promoter using a luciferase reporter assay and gel shift and ChIP studies. Our findings define a previously unidentified mechanism that Ca^{2+} influx via the $Ca_v3.2$ T-type Ca^{2+} channel regulates Sox9 expression through the calcineurin/NFAT signaling pathway during tracheal chondrogenesis.

Congenital tracheal malformations (CTMs), such as tracheal stenosis, are rare human conditions caused by defective development of the cartilaginous trachea (1, 2). Made of a series of imperfect rings interconnected by fibrous tissue, the trachea is flexible enough to bend yet rigid enough to remain widely patent during respiration. Each ring, with the exception of the cricoid cartilage (a true ring), is actually an arch that rests on the posterior membranous trachea, which separates the airway and esophagus. As might be expected from their functional importance, defects in the tracheal rings can compromise the airway lumen and lead to tracheal stenosis, a life-threatening condition (2, 3). The pathogenesis of the tracheal stenosis has not been elucidated.

The development of mouse trachea begins as a simple outpouching from ventral foregut endoderm at about embryonic day (E) 9.5 (4). The foregut is then further partitioned into the ventral trachea and the dorsal esophagus at E11.5 along the dorsoventral axis (5). Cartilage rings and smooth muscle of the trachea tube are differentiated from the trachea surrounding the splanchnic mesenchyme at E13.5–E15.5 (6, 7). Cartilage rings are formed by proliferation and then condensation of chondrogenic-committed mesenchymal cells. These condensed mesenchymal cells then differentiate into chondrocytes that express cartilage-specific proteins, such as type II collagen (Col2a1) (8).

The transcription factor sex determination region of Y chromosome (SRY)-related high-mobility group-Box gene 9 (Sox9) is involved in chondrogenesis, as well as sex determination, during embryonic development (9–11). Sox9 plays critical roles in each step of chondrogenesis and is expressed in chondrogenic progenitors and differentiated chondrocytes but not in hypertrophic chondrocytes (12–14). Mutation of the human *SOX9* gene causes a severe skeletal malformation syndrome called campomelic dysplasia (15). In mice, loss of one allele of Sox9 gene ($Sox9^{+/-}$) is perinatal-lethal because of severe bone malformation and respiratory deficiency. $Sox9^{+/-}$ mice also show abnormal cartilage formation, including tracheal cartilage (16). Interestingly, transgenic mice with overexpression of Sox9 driven by the *Col2a1* promoter showed chondrodysplasia due to inhibited chondrocyte proliferation (17). These studies demonstrate that Sox9 expression is crucial for normal development of cartilage and needs to be precisely regulated.

Voltage-gated Ca^{2+} channels (VGCCs) are key regulators of Ca^{2+} influx in many cell types, including chondrocytes and osteoblasts (18, 19), and Ca^{2+} influx is involved in the differentiation of chondrogenic mesenchymal cells into chondrocytes (20). $Ca_v3.2$ T-type and $Ca_v1.2$ L-type Ca^{2+} channels, but not other VGCCs, are regulated by 1,25-dihydroxyvitamin D3 in murine osteoblast cells (21), and these two channels are dynamically regulated in cartilage and bone during endochondral development (18). However, the roles of VGCCs, especially T-type Ca^{2+} channels, in tracheal chondrogenesis remain unclear.

T-type Ca^{2+} channels (Ca_v3 family) are involved in diverse physiological processes, such as hormone secretion, gene expression, cell proliferation and differentiation, and development of neuronal and cardiac diseases (22, 23). Three T-type Ca^{2+} channel subunits have been identified: $Ca_v3.1$, $Ca_v3.2$, and $Ca_v3.3$ (24).

Significance

The tracheal cartilage rings are important for protecting and maintaining the airway. However, the chondrogenesis of tracheal cartilage is not completely understood. We demonstrate that the $Ca_v3.2$ T-type calcium channel is required for normal tracheal cartilage ring formation. Calcium influx via $Ca_v3.2$ induces chondrogenesis and up-regulates a chondrogenic master gene, sex determination region of Y chromosome (SRY)-related high-mobility group-Box gene 9 (Sox9), via a calcium and calcineurin-dependent pathway. $Ca_v3.2$-dependent regulation of Sox9 is mediated by a newly identified nuclear factor of activated T-cell binding site on the Sox9 promoter. Our study provides novel insight into the roles of $Ca_v3.2$ T-type calcium channels in tracheal development. Moreover, *CACNA1H*, the human homolog of the mouse $Ca_v3.2$-encoding gene, may be a potential candidate gene involved in congenital tracheal stenosis in humans.

Author contributions: S.-S.L., B.-H.T., K.-R.L., and C.-C.C. designed research; S.-S.L. performed research; S.-S.L. contributed new reagents/analytic tools; S.-S.L., B.-H.T., and C.-C.C. analyzed data; and S.-S.L., R.J.H.S., K.P.C., and C.-C.C. wrote the paper.

The authors declare no conflict of interest.

This article is a PNAS Direct Submission. J.R.R. is a guest editor invited by the Editorial Board.

[1]To whom correspondence should be addressed. E-mail: ccchen@ibms.sinica.edu.tw.

This article contains supporting information online at www.pnas.org/lookup/suppl/doi:10.1073/pnas.1323112111/-/DCSupplemental.

Polymorphism or mutations of the human $Ca_v3.2$ gene are associated with childhood-absent epilepsy, idiopathic generalized epilepsy, and autism-spectrum disorders (25–27). $Ca_v3.2^{-/-}$ mice exhibit many abnormal phenotypes related to cardiovascular and neuronal functions (28–33). Here, we provide evidence to support the hypothesis that the $Ca_v3.2$ T-type Ca^{2+} channel is important in tracheal chondrogenesis via a calcineurin/nuclear factor of activated T cell (NFAT)/Sox9-dependent pathway.

Results

$Ca_v3.2^{-/-}$ Mice Show Abnormal Tracheal Development. Previously, we showed that mice lacking $Ca_v3.2$ demonstrated cardiac fibrosis due to abnormal relaxation of the coronary arteries (28). In addition, $Ca_v3.2^{-/-}$ mice emitted an intermittent, high-pitched chirping sound similar to the inspiratory stridor made by neonates with congenital tracheal stenosis (Movie S1). To explore the etiology of this noise in $Ca_v3.2^{-/-}$ mice, we conducted a detailed analysis of the airway. Compared with WT tracheas, which had a smooth appearance, tracheas from all $Ca_v3.2^{-/-}$ mice were narrow and elliptically shaped, with the long axis oriented in the anterior-posterior direction (Fig. S1*A*). Alcian blue staining showed that WT mice had continuous, distinct cartilaginous rings that resembled arches, whereas the cartilaginous rings of the $Ca_v3.2^{-/-}$ mice were frequently disrupted anteriorly, resembling an arch missing its keystone, thus collapsing the transverse diameter of the tracheal airway (Fig. 1*A*). The mean number of disrupted cartilaginous rings in adult $Ca_v3.2^{-/-}$ mice was 9.95 ± 0.51 ($n = 25$) vs. none in WT mice ($n = 20$). We also examined the cartilage ring pattern in the bronchi and found there is no difference between the WT and $Ca_v3.2^{-/-}$ mice (Fig. S1*B*). To determine whether the cartilage disruption was congenital, we examined tracheas from embryos and neonatal pups and found abnormal tracheal rings at both E14.5 and postnatal day 1, with no ring abnormalities in age-matched WT embryos and neonates (Fig. 1*A*). Almost all of the cartilage rings were disrupted in the $Ca_v3.2^{-/-}$ trachea at E14.5 and postnatal day 1. We also examined cricoid cartilage and cartilages from the xiphistemum, ear, nose, and articular cartilage and found no morphological difference between WT and $Ca_v3.2^{-/-}$ mice (Fig. S1*C*). It is unclear why only tracheal ring cartilage but not the other cartilages are affected in the $Ca_v3.2^{-/-}$ mice. One possibility is that $Ca_v3.2$ is differentially expressed in different cartilages. To test this possibility, we examined the expression of *$Ca_v3.2$* in different cartilages and found that *$Ca_v3.2$* is predominantly expressed in the tracheal cartilage rings and hardly detectable in the other cartilages (Fig. S2). The unique expression pattern of *$Ca_v3.2$* explains the tracheal-specific defects in $Ca_v3.2^{-/-}$ mice.

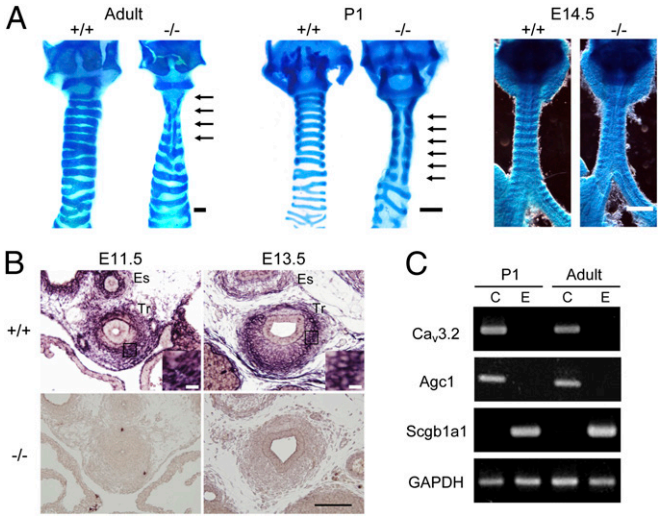

Fig. 1. $Ca_v3.2^{-/-}$ mice show abnormal tracheal development. (*A*) Alcian blue staining of WT and $Ca_v3.2^{-/-}$ cartilaginous rings in the tracheas of 12-wk-old mice (adult), postnatal day 1 mice (P1), and E14.5 embryos. Arrows indicate incomplete cartilage. (Scale bar: 300 μm.) (*B*) In situ hybridization of *$Ca_v3.2$* transcript in the developing trachea at E11.5 and E13.5, revealing expression on the ventrolateral side of $Ca_v3.2^{+/+}$ but not $Ca_v3.2^{-/-}$ tracheas. (*Insets*) Higher magnification of the area in the rectangles are shown. Es, esophagus; Tr, trachea. (Scale bars: 100 μm; *Insets*, 10 μm.) (*C*) RT-PCR analysis of *$Ca_v3.2$*, *Agc1*, and *Scgb1a1* mRNA levels in tracheal cartilage (C) and epithelium (E) from P1 mice and adult mice.

$Ca_v3.2$ Is Expressed in Tracheal Mesenchyme and Cartilage but Not Epithelium. During the early stages of chondrogenesis, the embryonic trachea is surrounded by a continuous layer of mesenchymal cells that condense at E14.5 to form segments (34). Our in situ hybridization results (Fig. 1*B*) showed *$Ca_v3.2$* expressed in chondrogenic mesenchymal cells on the ventrolateral sides of E11.5 and E13.5 WT but not $Ca_v3.2^{-/-}$ developing trachea. Importantly, *$Ca_v3.2$* was not expressed in the tracheal epithelium at E11.5 or E13.5 in WT mice (Fig. 1*B*). These observations were supported by RT-PCR analysis of *$Ca_v3.2$* transcripts in isolated cartilaginous rings and epithelia from neonatal and adult tracheas (Fig. 1*C*). In addition, RT-PCR revealed clear, tissue-specific expression of *aggrecan* (*Agc1*, a marker of chondrogenic cells) and *secretoglobin 1a1* [*Scgb1a1*, an epithelium marker (35)] in tracheal cartilage and the epithelium, respectively, which indicates no cross-contamination of tissues (Fig. 1*C*). The temporal and spatial expression patterns of *$Ca_v3.2$* transcripts suggest that the CTM in $Ca_v3.2^{-/-}$ mice resulted from abnormal chondrogenesis.

$Ca_v3.2$ Up-Regulates Chondrogenic Markers and Enhances Chondrogenesis in ATDC5 Cells. Because *$Ca_v3.2$* transcripts were expressed in chondrogenic mesenchymal cells of E13.5 WT mice (Fig. 1*B*), $Ca_v3.2$ may be involved in regulating chondrogenic differentiation. Therefore, we expressed $Ca_v3.2$ in the murine chondrogenic cell line ATDC5, which is often used to assess chondrogenesis in vitro (36). ATDC5 cells expressed $Ca_v1.2$ but not Ca_v3 channels (Fig. S3*A*). After expression of $Ca_v3.2$ in ATDC5 cells, typical low-voltage activated calcium currents can be recorded (Fig. S3 *B* and *C*), indicating that functional $Ca_v3.2$ T-type Ca^{2+} channels were expressed in transfected ATDC5 cells. Alcian blue staining revealed greater chondrogenic differentiation in $Ca_v3.2$-transfected ATDC5 cells than negative control cells (Fig. 2*A*). To support further our hypothesis that $Ca_v3.2$ plays a role in chondrogenic differentiation, we blocked Ca^{2+} influx into ATDC5 cells via T-type Ca^{2+} channels by using NNC 55-0396 (37). This treatment blocked enhancement of chondrogenic differentiation in $Ca_v3.2$-transfected ATDC5 cells but not control cells (Fig. 2*A*). $Ca_v3.2$ overexpression significantly increased the mRNA levels of chondrogenic marker genes *Sox9*, *Agc1*, and *Col2a1* in ATDC5 cells, which could be inhibited by the addition of NNC 55-0396 (Fig. 2*B*). The reduced percentages of *Sox9*, *Agc1*, and *Col2a1* by NNC 55-0396 in $Ca_v3.2$-transfected ATDC5 cells are similar (68 ± 3.6%, 63 ± 3.2%, and 65 ± 2.6%, respectively). To test whether the above-described effects in an established cell line are conserved in embryonic cells, we established high-density micromass cell cultures of embryonic limb bud mesenchymal cells from WT and $Ca_v3.2^{-/-}$ embryos. $Ca_v3.2^{-/-}$ mesenchymal cells were able to undergo chondrogenic differentiation, but to a much less extent compared with WT mesenchymal cells (Fig. 2*C*). Notably, treatment with NNC 55-0396 reduced chondrogenic differentiation in WT cells but did not affect the process further in $Ca_v3.2^{-/-}$ cells. To confirm our observation of the positive association of $Ca_v3.2$ levels and chondrogenic differentiation, we used another T-type Ca^{2+} channel blocker, mibefradil, and obtained results similar to those for NNC 55-

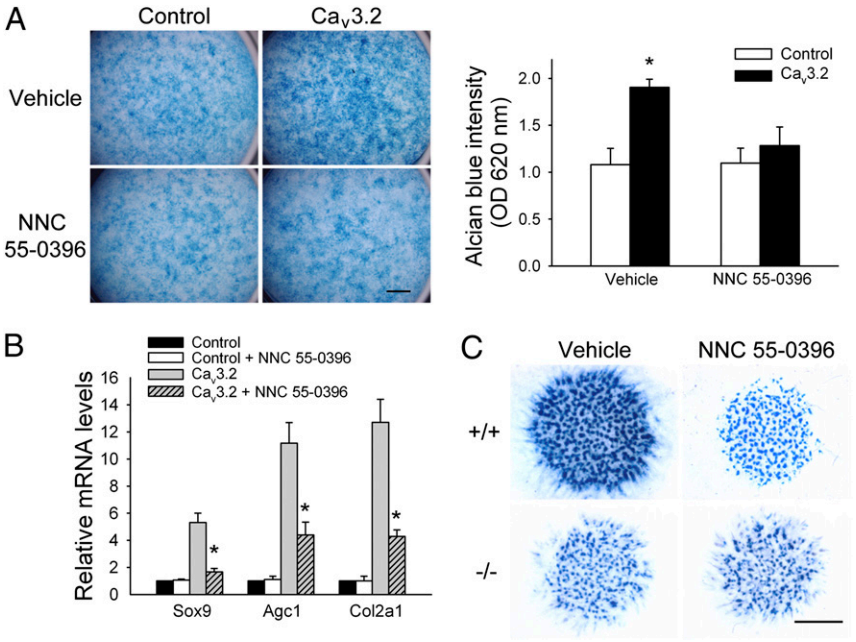

Fig. 2. $Ca_v3.2$ enhances chondrogenesis in ATDC5 cells. (*A*) Alcian blue staining and quantification of cartilage nodules formed in ATDC5 cells transfected with control or $Ca_v3.2$ plasmids and then treated with NNC 55-0396 (5 μM) or vehicle for 12 d ($n = 6$ for each group). (Scale bar: 2 mm.) *$P < 0.05$, compared with control. (*B*) Real-time PCR analysis of *Sox9*, *Agc1*, and *Col2a1* mRNA expression in ATDC5 cells transfected with control or $Ca_v3.2$ plasmids and then treated with NNC 55-0396 or vehicle for 9 d ($n = 8$ for each group). *$P < 0.05$, compared with $Ca_v3.2$. (*C*) Micromass cultures of mesenchymal cells from E11.5 WT and $Ca_v3.2^{-/-}$ mouse limbs treated with vehicle or NNC 55-0396 for 9 d. (Scale bar: 2 mm.)

0396 in both WT and $Ca_v3.2^{-/-}$ cells (Fig. S4*A*). Reexpression of $Ca_v3.2$ in primary chondrocytes isolated from $Ca_v3.2^{-/-}$ pups also significantly increased the mRNA levels of *Sox9*, *Agc1*, and *Col2a1* (Fig. S4*B*). Thus, in both ATDC5 and embryonic mesenchymal cells, Ca^{2+} influx via $Ca_v3.2$ up-regulates the expression of chondrogenic markers and promotes chondrogenic differentiation.

$Ca_v3.2$ Enhances Chondrogenesis in a Calcineurin/NFAT-Dependent Manner. We previously showed that Ca^{2+} influx via $Ca_v3.2$ activates the calcineurin/NFAT signaling pathway, which then induces pathological cardiac hypertrophy (29). Moreover, signaling by the calcineurin/NFAT pathway can induce chondrogenesis in vitro (38). In addition, we have recently shown that $Ca_v3.2$ regulates the calcineurin/NFAT pathway through both Ca^{2+} influx and calcineurin binding (39). Thus, we hypothesized that Ca^{2+} influx via $Ca_v3.2$ activates the calcineurin/NFAT signaling pathway to induce tracheal chondrogenesis. To test this hypothesis, we investigated the effects of the calcineurin inhibitor cyclosporin A (CsA) on the chondrogenic differentiation of ATDC5 cells with and without $Ca_v3.2$ overexpression. CsA attenuated the expected enhancement of $Ca_v3.2$-induced chondrogenic differentiation but had little effect on control cells (Fig. 3*A*). Quantification of Alcian blue staining showed a 46% reduction in the CsA-treated, $Ca_v3.2$-overexpressing cells compared with control cells (Fig. 3*A*; $P < 0.05$). In addition, the expression of chondrogenic marker genes was significantly reduced in CsA-treated, $Ca_v3.2$-overexpressing ATDC5 cells but not their control counterparts (Fig. 3*B*). The reduced percentages of *Sox9*, *Agc1*, and *Col2a1* by CsA in $Ca_v3.2$-transfected ATDC5 cells are similar (62 ± 2.8%, 58 ± 3.3%, and 55 ± 3.5%, respectively), indicating the regulation of *Sox9*, *Agc1*, and *Col2a1* is likely dependent on the same calcineurin/NFAT signaling pathway.

We also crossed $Ca_v3.2^{-/-}$ mice with NFAT-luciferase (Luc) reporter transgenic mice (40) to generate $Ca_v3.2^{+/-}$/NFAT-Luc and $Ca_v3.2^{-/-}$/NFAT-Luc mice. Luc activity was lower (by 5.6-fold; $P < 0.005$) in tracheas from $Ca_v3.2^{-/-}$/NFAT-Luc mice than $Ca_v3.2^{+/-}$/NFAT-Luc mice at E15.5 (Fig. 3*C*). As expected, the expression of Luc was lower in tracheal rings of $Ca_v3.2^{-/-}$/NFAT-Luc mice than $Ca_v3.2^{+/-}$/NFAT-Luc mice at E14.5 (Fig. 3*D*). Thus, the ATDC5 chondrogenesis assay and the transgenic model provide evidence to support our hypothesis that Ca^{2+} influx via $Ca_v3.2$ activates the calcineurin/NFAT signaling pathway to induce tracheal chondrogenesis.

$Ca_v3.2^{-/-}$ Mice Exhibit Reduced Sox9, Agc1, and Col2a1 Expression. Sox9, one of the earliest markers of committed chondrogenic cells, is essential for early differentiation of chondrogenic cells (14). Therefore, we examined the effect of the $Ca_v3.2$ null mutation on chondrogenic differentiation by assessing Sox9 expression. Sox9 protein was expressed on the ventrolateral sides of the tracheal tube at E11.5 and E13.5 in both WT and $Ca_v3.2^{-/-}$ mice (Fig. 4*A*). However, the Sox9 signal was significantly weaker in $Ca_v3.2^{-/-}$ trachea than WT trachea at both E11.5 and E13.5 (Fig. 4*A*), even though the total number of mesenchymal cells at E11.5 was similar in WT and $Ca_v3.2^{-/-}$ embryos (568 ± 33 and 566 ± 34, respectively). The reduced expression of Sox9 was observed throughout the embryonic $Ca_v3.2^{-/-}$ tracheal tube (Fig. S5). Furthermore, in vivo BrdU labeling of E13.5 embryos revealed no difference in the number of proliferating $Sox9^+$ mesenchymal cells (Fig. S6*B*). There is also no significant difference in the proliferating cell nuclear antigen-positive cells (Fig. S6*A*). A TUNEL assay also showed no difference in the apoptosis of embryonic WT and $Ca_v3.2^{-/-}$ tracheas at E13.5 (Fig. S6*C*). Thus, $Ca_v3.2$ may be an important modulator for Sox9 expression but not for mesenchyme cell proliferation or apoptosis during chondrogenesis in the trachea.

A certain level of Sox9 expression is essential for the condensation of chondroprogenitor cells into segments along developing trachea at E14.5 (14, 34). Sox9-positive cells formed a clear banding pattern on the ventral side of developing trachea in WT but not $Ca_v3.2^{-/-}$ mice (Fig. 4*B*). The reduced Sox9-positive banding in $Ca_v3.2^{-/-}$ mice may be due to a specific loss of Sox9 expression, impaired mesenchymal condensation during tracheal

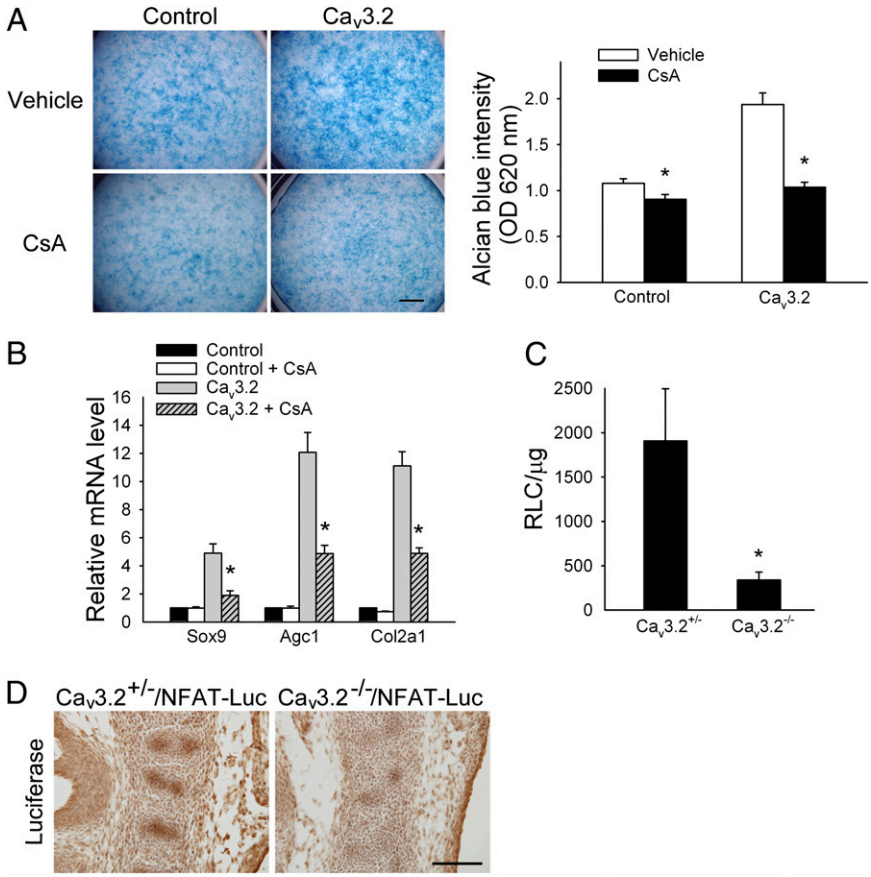

Fig. 3. $Ca_v3.2$ enhances chondrogenesis in a calcineurin/NFAT-dependent manner. (*A*) Alcian blue staining and quantification of cartilage nodules formed in ATDC5 cells transfected with control or $Ca_v3.2$ plasmids with and without CsA (2.5 μM for 12 d, $n = 5$ for each group). (Scale bar: 2 mm.) $^*P < 0.05$, compared with vehicle. (*B*) Real-time PCR analysis of mRNA levels of *Sox9*, *Agc1*, and *Col2a1* in transfected ATDC5 cells treated with CsA (2.5 μM) or vehicle for 9 d ($n = 8$ for each group). $^*P < 0.05$, compared with $Ca_v3.2$. (*C*) NFAT-Luc reporter analysis of tracheal tubes from $Ca_v3.2^{-/-}$/NFAT-Luc and $Ca_v3.2^{+/-}$/NFAT-Luc embryos at E15.5. Data are the relative luciferase activity (RLU) per microgram of protein of the indicated tissue lysate ($n = 3$ for each group). $^*P < 0.05$, compared with $Ca_v3.2^{+/-}$. (*D*) Immunohistochemical staining of Luc expression in longitudinal sections of tracheal tubes of $Ca_v3.2^{-/-}$/NFAT-Luc and $Ca_v3.2^{+/-}$/NFAT-Luc embryos at E14.5. (Scale bar: 100 μm.)

cartilage development, or both. Thus, we examined the expression pattern of another mesenchymal cell marker, paired-related homeobox gene-1 (Prx1) in embryonic tracheas (41, 42). Prx1 is a homeobox-containing gene that is expressed in the mesenchymal cells differentiating into facial, limb, and vertebrate skeleton during embryogenesis (41). In limb bud mesenchymal cells, the expression of Prx1 preceded that of Sox9 (42). Our results showed that Prx1-positive cells also formed a clear banding pattern on the ventral side of developing trachea in WT mice and a disrupted banding pattern in $Ca_v3.2^{-/-}$ mice (Fig. 4*B*). Interestingly, the staining intensity of Prx1 in each prechondrogenic condensate was similar in both WT and $Ca_v3.2^{-/-}$ tracheas (Fig. 4*B* and Fig. S7). These results show that lack of $Ca_v3.2$ indeed affects the condensation of chondroprogenitor cells but not the expression of Prx1.

Sox9 regulates many chondrogenic marker genes, such as Agc1 and Col2a1 (43, 44), and, indeed, the expression of both of these proteins was decreased in E16.5 $Ca_v3.2^{-/-}$ trachea (Fig. 4*C*) (45). Reduced Sox9 expression in $Ca_v3.2^{-/-}$ trachea may lead to abnormal tracheal segmentation and reduced expression of markers of chondrogenesis.

$Ca_v3.2$ Up-Regulates Sox9 Expression in a Calcineurin/NFAT-Dependent Manner. Given the similar expression patterns for $Ca_v3.2$ and Sox9 during early tracheal development, the reduced Sox9 expression in $Ca_v3.2^{-/-}$ tracheas, and the involvement of the calcineurin/NFAT signaling pathway in $Ca_v3.2$-dependent chondrogenesis, we hypothesized that Ca^{2+} influx via $Ca_v3.2$ may regulate the expression of Sox9 during tracheal chondrogenesis, perhaps through NFAT signaling. An earlier study of human *SOX9* showed an essential promoter region located ~750 bp upstream of the transcription start site (46). We thus generated a construct that contains the equivalent mouse *Sox9* sequence, from −735 to +53 bp, fused to a Luc reporter (−735-Luc) and generated serial 5′-deletions using this construct. It has been shown that increasing the extracellular Ca^{2+} concentration to 10 mM can induce Ca^{2+} influx via the $Ca_v3.2$ window currents at the resting membrane potential in nonexcitable cells (29, 39, 47). Our positive control experiment demonstrated that the NFAT-response element (RE)-Luc reporter could be activated in a $Ca_v3.2$-dependent manner by increasing extracellular Ca^{2+} concentration in ATDC5 cells (Fig. 5*A*). Using this approach, we identified the $Ca_v3.2$-dependent fragment (from −499 to −312 bp) from which expression could be induced in calcium-treated $Ca_v3.2$-transfected ATDC5 cells (Fig. 5*A*). The $Ca_v3.2$-dependent induction of −499-Luc reporter activity could be inhibited by treatment with NNC 55-0396, FK506, and CsA (Fig. 5*B*). To confirm that Sox9 expression is regulated by NFAT, we expressed EGFP-NFATc4 in ATDC5 cells and found induced Sox9 expression (Fig. S8). Coexpression of EGFP-NFATc4 also increased the reporter activity of −499-Luc (Fig. 5*C*).

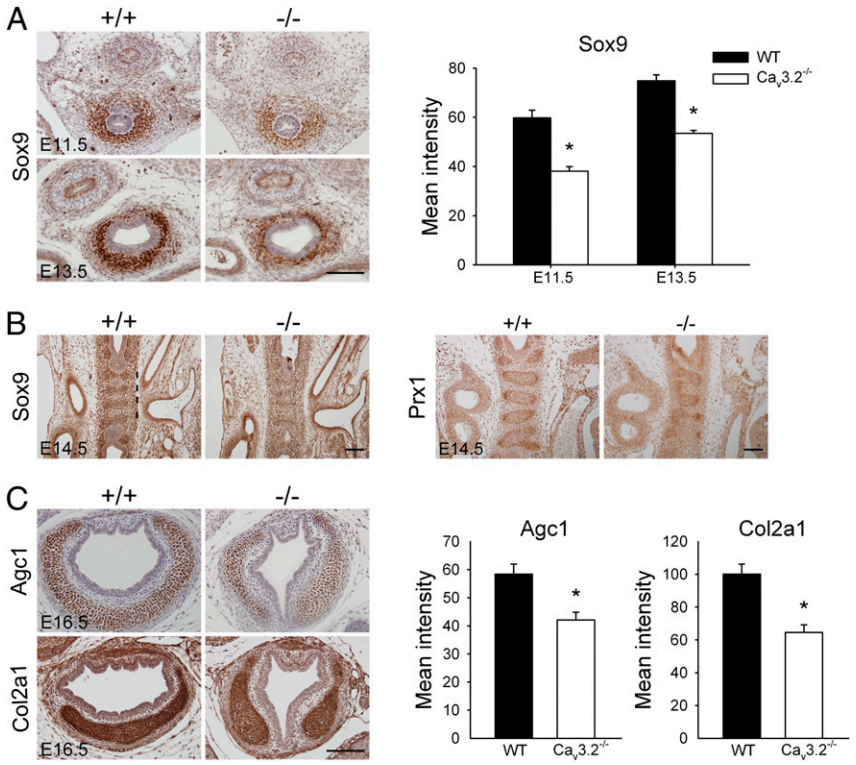

Fig. 4. $Ca_v3.2^{-/-}$ mouse embryos show reduced Sox9, Agc1, and Col2a1 expression. (*A*) Immunohistochemical staining and quantification of Sox9 expression on the ventrolateral side of the developing trachea from E11.5 ($n = 5$) and E13.5 ($n = 6$) WT and $Ca_v3.2^{-/-}$ mice. *$P < 0.05$, compared with WT. (*B*) Immunohistochemical staining of Sox9 and Prx1 expression in the longitudinal middle sections of developing tracheas. Vertical lines indicate the location of segments. (*C*) Immunohistochemical staining and quantification of Agc1 ($n = 5$) and Col2a1 ($n = 6$) expression in E16.5 WT and $Ca_v3.2^{-/-}$ tracheas. *$P < 0.05$, compared with the WT. (Scale bar: 100 μm.)

Therefore, the *Sox9* promoter region between −499 and −312 bp may be important for NFAT binding and $Ca_v3.2$ regulation. Using PROMO software (48), we identified a putative NFAT binding site (TTTCC, −489 to −485 bp) upstream of the *Sox9* transcription start site and showed that mutations within this site (mut1 and mut2) abolished the NFAT dependence, as well as the $Ca_v3.2$ dependence, on the induction of −499-Luc reporter activity (Fig. 5 *C* and *D*). To confirm the interaction between NFAT and the putative NFAT binding site on the *Sox9* promoter, we used an EMSA with a digoxigenin (DIG)-labeled oligonucleotide (−502 to −474 bp) as a probe. Lysates from EGFP-NFATc4 but not EGFP-transfected cells showed several shifted bands (Fig. 6*A*). The shifted bands disappeared in the presence of excess unlabeled WT probe, but the upper band, which represents the NFAT–*Sox9* DNA complex, remained, with the addition of an excess of unlabeled mutant probes unable to bind NFAT (mut1 or mut2). Therefore, the putative NFAT binding site is essential for the interaction between NFAT and the Sox9 promoter. An anti-GFP antibody could supershift the NFAT–*Sox9* promoter complex (Fig. 6*A*). Thus, NFAT could bind to the TTTCC sequence of the mouse *Sox9* promoter.

To demonstrate that NFAT binds to the *Sox9* promoter in vivo, we used a ChIP assay to examine enrichment of 227 bp containing the NFAT binding sequences in *Sox9* promoter pulled down with EGFP-NFATc4 in ATDC5 cells. Compared with the EGFP control, the precipitated product with EGFP-NFATc4 showed a significantly enriched 227 bp of Sox9 promoter detected by PCR or real-time PCR (Fig. 6 *B* and *C*). Combined with the fact that overexpressing NFAT increased *Sox9* expression (Fig. S8), as well as with the results of EMSA experiments (Fig. 6*A*) and Luc reporter assays (Fig. 5), these results suggest that NFAT regulates Sox9 expression by binding to the TTTCC sequence of the mouse *Sox9* promoter.

Discussion

Although many molecules are involved in chondrogenesis (49), little is known about the role of VGCCs in this process. T-type Ca^{2+} channels are highly expressed in many developing tissues and are implicated in regulating cellular events leading to cell proliferation and differentiation (50). Calcium influx through T-type Ca^{2+} channels activates several cellular pathways, including calcineurin/NFAT (29, 39), extracellular signal-regulated kinase (31, 51–53), nitric oxide synthase 3 (54), and Ca^{2+}/calmodulin-dependent protein kinase II (55). However, the detailed mechanisms linking these T-type Ca^{2+} channel-activated signaling pathways to cell proliferation and differentiation are not completely clear. Interestingly, $Ca_v3.1$ is mostly linked to cell proliferation, whereas $Ca_v3.2$ is implicated in cell differentiation. $Ca_v3.1$ is involved in cell proliferation of smooth muscle cells (56–58), tumor cells (59, 60), and preadipocytes (61), but $Ca_v3.2$ is implicated in the differentiation of human skeletal muscle (62), neuritogenesis of neuroblastoma cells (63, 64), and neuroendocrine differentiation of prostate cancer cells (65). In line with these studies, our data demonstrated that $Ca_v3.2$ is involved in tracheal chondrogenic differentiation but not proliferation or apoptosis of tracheal mesenchymal cells (Fig. S6). $Ca_v3.2^{-/-}$ mice did not show abnormal morphogenesis in cartilage other than trachea (Fig. S1*C*). The trachea-specific cartilage defects in $Ca_v3.2^{-/-}$ mice are probably caused by the differential expression of $Ca_v3.2$ in different cartilages, as shown in Fig. S4. We could not detect the expression of the other two T-type Ca^{2+} channels, $Ca_v3.1$ and $Ca_v3.3$, in different cartilages isolated from WT and $Ca_v3.2^{-/-}$ mice, which rules out the possible compensatory effect by other Ca_v3 T-type Ca^{2+} channels.

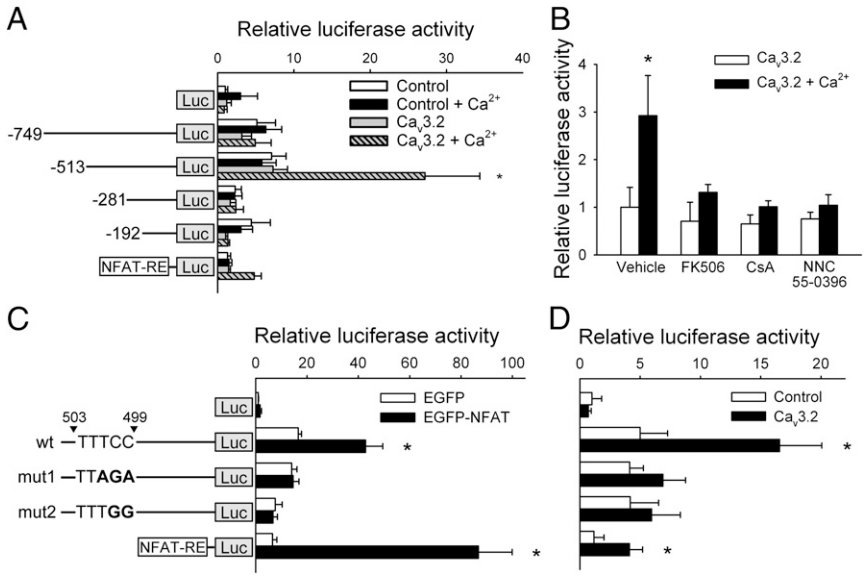

Fig. 5. $Ca_v3.2$ up-regulates *Sox9* expression in a calcineurin/NFAT-dependent manner. (*A*) Deletion analysis of the *Sox9* promoter in ATDC5 cells transfected with control or $Ca_v3.2$ plasmids and then treated with 10 mM $CaCl_2$. The $Ca_v3.2$-dependent promoter site was located between −499 and −312 bp. The NFAT-RE-Luc reporter was a positive control ($n = 4$ for each group). *$P < 0.05$, compared with the other treatments and using the same reporter. (*B*) Effect of FK506 (2.5 μM), CsA (2.5 μM), and NNC 55-0396 (5 μM) treatment on ATDC5 cells transfected with the −499-Luc reporter plasmid ($n = 5$ for each group). *$P < 0.05$, compared with $Ca_v3.2$. (*C*) Luc reporter analysis of pGL3, −499-Luc (wt), mutated −499-Luc (mut1, mut2), and NFAT-RE-Luc reporters in ADTC5 cells transfected with EGFP or EGFP-NFAT plasmid ($n = 4$ for each group). *$P < 0.05$, compared with the EGFP group. (*D*) Luc reporter analysis in ADTC5 cells transfected with control or $Ca_v3.2$ plasmids and with 10 mM $CaCl_2$ ($n = 5$ for each group). *$P < 0.05$, compared with the control group.

The ATDC5 cell line is often used as a cellular model to assess chondrogenesis in vitro (36). $Ca_v3.2$ T-type Ca^{2+} channels can be detected by a specific $Ca_v3.2$ antibody in ATDC5 cells (18). However, we could not detect the presence of $Ca_v3.2$ in ATDC5 cells using either RT-PCR (Fig. S3*A*) or the whole-cell patch-clamp technique (Fig. S3*B*). Under our recording condition, both T-type and L-type Ca^{2+} channels can be activated and recorded if present. Even though the transcript of $Ca_v1.2$ can be detected in ATDC5 cells (Fig. S3*A*), we cannot detect the calcium influx via L-type Ca^{2+} channels (Fig. S3*B*). These results suggest that in our culture condition, ATDC5 cells did not express detectable T-type or L-type Ca^{2+} channels using an electrophysiological technique.

VGCCs are encoded by 10 different genes ($Ca_v1.1$–$Ca_v1.4$, $Ca_v2.1$–$Ca_v2.3$, and $Ca_v3.1$–$Ca_v3.3$) (66); however, to our knowledge,

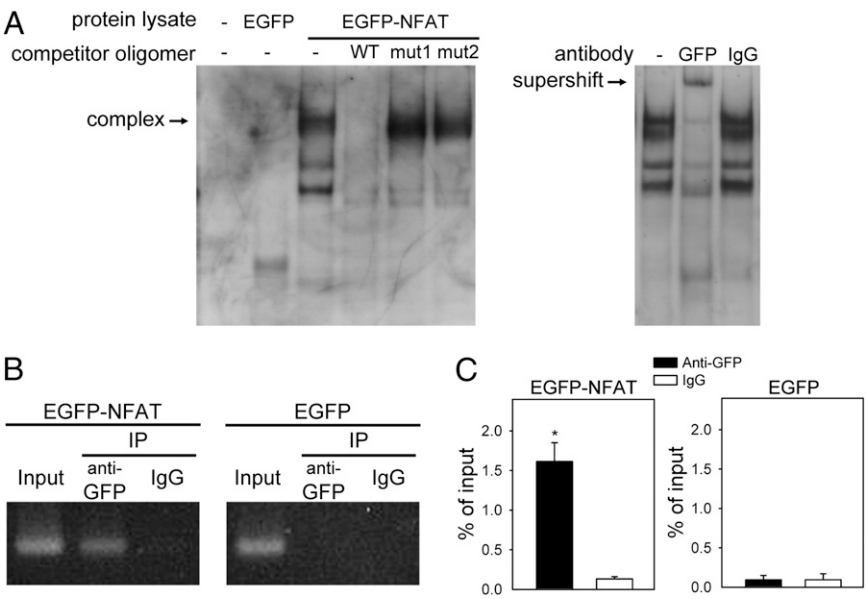

Fig. 6. NFAT binds to the promoter region of Sox9 in ATDC5 cells. (*A*, *Left*) EMSA with mouse *Sox9* promoter region −502 to −474 bp used as a probe in the detection of NFAT–*Sox9* DNA complex in lysates from EGFP-NFAT4–transfected but not EGFP-transfected cells. (*A*, *Right*) Supershift of NFAT–*Sox9* DNA complex induced by anti-GFP but not IgG antibody. (*B*) ChIP assay of anti-EGFP antibody or control rabbit IgG in ATDC5 cells transfected with EGFP-NFAT or EGFP plasmid. DNA immunoprecipitated by anti-EGFP antibody was amplified by PCR to detect the *Sox9* fragment containing the NFAT binding site. A 10-fold dilution was used in the input lanes. (*C*) Quantification of real-time PCR from ChIP assay ($n = 4$). *$P < 0.05$, compared with the IgG group.

only $Ca_v3.2^{-/-}$ mice display abnormal tracheal malformation. In addition to VGCCs, other calcium-permeable channels, such as NMDA receptor (67, 68), Orai 1 (69), acid-sensing ion channel (70), and transient receptor potential (TRP) (71) channels, are identified in chondrocytes. The role of these channels in chondrocytes is not completely understood. TRPV4-mediated Ca^{2+} influx is involved in transmitting the mechanotransduction signals to increased ECM production (72). The TRPV4 channel is important for osmotically activated Ca^{2+} signaling in articular chondrocytes, and lack of TRPV4 in mice leads to progressive increases in bone density and joint degradation (73). However, it has not been reported that these channels are involved in tracheal chondrogenesis. These results support the idea that $Ca_v3.2$ plays a specific role in regulating the development of tracheal cartilage rings.

One may argue that the abnormal tracheal phenotype in the $Ca_v3.2^{-/-}$ mice is because of a closure failure of the tracheal rings rather than a problem with cartilage formation. If the tracheal rings are formed by migration of chondrocytes from the bilateral sides to the ventrocentral part of the trachea, we would expect to observe a temporary gap in the cartilage ring during development in WT trachea. However, we never observed a broken Alcian blue staining pattern in the WT trachea. The earliest time point when Alcian blue staining could be observed was E14.5, with a clear cartilage banding pattern (Fig. 1*A*). In addition, immunostaining of Sox9 and Prx1 showed a clear banding pattern on the ventrocentral part of the WT trachea at E14.5 (Fig. 4). Immunostaining of Sox9 on the cross-section of the WT trachea at E13.5 also showed continuous staining on the ventrocentral part of the tracheal tube (Fig. 4 and Fig. S5). These data suggest that during normal tracheal cartilage development, the cartilaginous rings are formed by mesenchymal cells differentiated from the condensed mesenchymal cells surrounding the tracheal tube but not by chondrocytes migrating from the ventrolateral side of the tracheal tube. Thus, the abnormal tracheal phenotype in the $Ca_v3.2^{-/-}$ mice most likely resulted from defective cartilage formation rather than closure of the tracheal rings resulting from migration or patterning defects.

The transcription factor Sox9 plays important roles in sex determination and chondrogenesis during development (9–11). During chondrogenesis, Sox9 is required for mesenchymal cell condensation and the expression of cartilage-specific ECM genes, including *Col2a1, Col11a2*, and *Agc1* (11, 14, 43, 44, 74). Even though Sox9 is crucial in chondrogenesis, its regulation remains unclear, and only a few transcriptional factors were found to regulate Sox9 expression directly. For example, Sp1, the cyclic-AMP response element binding protein, NF-κB, and CCAAT binding factor can bind to the promoter region of *Sox9* and promote its expression in chondrocytes (75–77). We identified an NFAT binding motif (TTTCC) in the mouse *Sox9* promoter that was required for $Ca_v3.2$-dependent Sox9 regulation on Luc reporter assay. In addition, NFAT directly bound to the identified sequence on gel shift, supershift, and ChIP assays. In agreement with our results, the calcineurin/NFAT signaling pathway induced chondrogenesis in vitro (38) and constitutively active NFAT induced the expression of Sox9 in C17 chondroprogenitor cells (78). SOX9 haploinsufficiency results in a lethal skeletal malformation syndrome called campomelic dysplasia in humans (15). Disruption of Sox9 also leads to perinatal lethality in heterozygous mice (11, 14). These results show that a 50% reduction of Sox9 already leads to a lethal phenotype in humans and mice. In mice lacking sonic hedgehog, the level of Sox9 is almost absent at the time of chondrogenesis, resulting in the failure of tracheal cartilage formation (34). The reduced percentage of Sox9 in $Ca_v3.2^{-/-}$ trachea (Fig. 4) is around 30%; in $Ca_v3.2^{-/-}$ mice, this reduction is enough to lead to malformation of the tracheal cartilage ring but not severe enough to cause a lethal phenotype.

In humans, CTMs can be observed in several disorders (79) [e.g., Pfeiffer syndrome (80), Goldenhar's syndrome (81), atelosteogenesis type 1 (82)]. The molecular mechanism leading to CTMs is not understood and is believed to be multifactorial. CTMs have been described in mice lacking genes involved in embryonic development [e.g., sonic hedgehog (6), Wnt (83, 84), bone morphogenetic protein (85, 86), FGFs (87, 88)]. Recently, mice with cartilage-specific deletion of Dicer 1 showed abnormal tracheal development because of a lack of ECM deposition (89). Most of these mutant mice die embryonically or shortly after birth because of the severe and complicated embryonic defects. We are the first, to our knowledge, to show that VGCCs are involved in the development of tracheal cartilage. Mice lacking chloride channels, cystic fibrosis transmembrane conductance regulator (CFTR) (90), or transmembrane protein 16A (TMEM16A) (7) also show abnormal tracheal cartilaginous rings; however, the tracheal cartilage defects in $CFTR^{-/-}$ and $TMEM16A^{-/-}$ mice may be secondary to defects in the tracheal epithelium (7, 90). Hence, our study provides novel insight into the roles of $Ca_v3.2$ T-type Ca^{2+} channels in tracheal development. Moreover, *CACNA1H*, the human homolog of the mouse $Ca_v3.2$-encoding gene, may be a potential candidate gene involved in congenital tracheal stenosis in humans.

Materials and Methods

Animals. All research conformed to National Institutes of Health guidelines and those of the Institutional Animal Care and Utilization Committee, Academia Sinica. $Ca_v3.2^{-/-}$ and NFAT-Luc mice were generated as described (28, 40). For analyses of embryonic trachea, 129SVJ $Ca_v3.2^{-/-}$ mice were bred into an imprinting control region (ICR) background for two generations. $Ca_v3.2^{+/-}$ (129/ICR) mice were used to generate the littermate $Ca_v3.2^{+/+}$ and $Ca_v3.2^{-/-}$ embryos used in this study. $Ca_v3.2^{+/-}$/NFAT-Luc mice were bred to $Ca_v3.2^{-/-}$ mice to generate $Ca_v3.2^{+/-}$/NFAT-Luc and $Ca_v3.2^{-/-}$/NFAT-Luc mice.

In Vitro Chondrogenesis. ATDC5 cells were grown and maintained in a 1:1 mixture of DMEM/F-12 medium with 5% (vol/vol) FBS. Chondrogenic differentiation was induced by plating ATDC5 cells at 5.0×10^4 cells in 12-well plates with insulin, transferrin, and sodium selenite supplement for 12 d as described (36). ATDC5 cells transfected with $Ca_v3.2$ or control plasmid (pcDNA3) using a Neon Transfection System (Invitrogen) were selected with 600 μg/mL G418, and the medium was changed every other day for 2 wk. During induction of chondrogenesis, the G418 concentration was reduced to 60 μg/mL. For micromass chondrogenesis, the limb mesenchymal cells in 2:3 DMEM/Ham F-12 medium containing 10% (vol/vol) FBS were cultured at a density of 1×10^7 cells/mL as described (38). ATDC5 and micromass cultures were changed every other day until harvesting and were supplemented with DMSO (vehicle), $CaCl_2$ (10 mM), FK506 (2.5 μM, a calcineurin inhibitor), CsA (2.5 μM), NNC 55-0396 (5 μM), or mibefradil (10 μM). Alcian blue (Sigma) staining, RNA isolation, quantitative RT-PCR, and the Luc reporter assay are described in *SI Materials and Methods*.

In Situ Hybridization. In situ hybridization of paraffin sections was done as previously described (91), using a DIG-labeled RNA system (Roche). A *$Ca_v3.2$*-specific probe was generated by RT-PCR and subcloned into pBluescript II Kpn 1/Sac I plasmid. Anti–DIG-alkaline phosphatase antibody was used to detect the RNA probe, and color was developed by use of nitro blue tetrazolium/5-bromo-4-chloro-3-indolyl-phosphate.

Immunohistochemistry. Paraffin sections (5 μm) were deparaffinized by boiling in 0.01 M sodium citrate, blocked in 3% (vol/vol) goat serum, and incubated with primary antibody overnight at 4 °C. Sections were then rinsed with PBS and incubated with biotinylated secondary antibody (1:200 dilution; Vector Labs) for 60 min. The antigen/antibody complexes were detected by sequential use of kits for detection of avidin/biotin complex (Vector Labs) and diaminobenzidine (Vector Labs). The following primary antibodies were used: anti-Sox9 and rabbit polyclonal anti-Luc (Santa Cruz Biotechnology), anti-Agc1 (Millipore), anti-Col2a1 (Abcam), and anti-Luc (Santa Cruz Biotechnology). The immunostaining intensities of Sox9, Agc1, and Col2a1 were analyzed using a HistoQuest system (TissueGnostics). Sox9-positive cells around the tracheal tube at E11.5 were counted as mesenchymal cells.

EMSA. Synthetic oligonucleotides containing the NFAT binding site of Sox9 and the complementary oligonucleotide were 3′ end-labeled with the use of DIG-11-ddUTP (Roche) and terminal transferase (New England Biolabs)

following the manufacturers' instructions and then annealed. The probes were incubated for 20 min at room temperature with 10 μg of HEK cell lysates containing the EGFP or EGFP-NFATc4 protein; 1 μg of poly(deoxyinosinic-deoxycytidylic) acid; and 0.1 μg of poly L-lysine in buffer containing 20 mM Hepes-KOH (pH 7.6), 1 mM EDTA, 10 mM $(NH4)_2SO_4$, 1 mM DTT, 0.2% Tween 20, and 30 mM KCl. For the competition assay, unlabeled WT or mutant-annealed oligonucleotide was added at 125-fold excess for 10 min at room temperature before the probe was added. For analysis of supershift induction, 8 ng of GFP antibody (monoclonal anti-GFP; Sloan–Kettering Cancer Center) was added for 20 min at room temperature before the probe was added. The reaction products were analyzed on 6% nondenaturing polyacrylamide gel.

ChIP Assay. A total of 6×10^6 ATDC5 cells were used for each immunoprecipitation as described earlier (92). Rabbit anti-GFP antibody (ChIP grade; Abcam) or control rabbit IgG (Sigma) was used for immunoprecipitation. DNA was purified and amplified by real-time quantitative PCR (qPCR). Data were expressed as the percentage of input DNA associated with immunoprecipitated GFP relative to the input chromatin. Oligonucleotides sequences used for RT-PCR, in situ hybridization, EMSA, ChIP and qPCR assays are listed in Table S1.

Statistical Analysis. Data are presented as mean ± SEM. Statistical analysis involved the Student *t* test or one-way ANOVA for more than two sample groups and Tukey's post hoc analysis. $P < 0.05$ was considered statistically significant.

ACKNOWLEDGMENTS. We thank Y.-C. Chen for assistance and the Pathology Core and Common Facilities Core Laboratory at the Institute of Biomedical Sciences (Academia Sinica). This work was supported by Grants 98-2320-B-001-017-MY3 and 100-2311-B-001-002-MY3 from the National Science Council, Taiwan (to C.-C.C.) and Grant AS100-CDA-L05 from the Academia Sinica (to C.-C.C.).

1. Carden KA, Boiselle PM, Waltz DA, Ernst A (2005) Tracheomalacia and tracheobronchomalacia in children and adults: An in-depth review. *Chest* 127(3):984–1005.
2. Phipps LM, Raymond JA, Angeletti TM (2006) Congenital tracheal stenosis. *Crit Care Nurse* 26(3):60–69.
3. Rutter MJ, Willging JP, Cotton RT (2004) Nonoperative management of complete tracheal rings. *Arch Otolaryngol Head Neck Surg* 130(4):450–452.
4. Que J, Choi M, Ziel JW, Klingensmith J, Hogan BL (2006) Morphogenesis of the trachea and esophagus: Current players and new roles for noggin and Bmps. *Differentiation* 74(7):422–437.
5. Perl A-KT, Wert SE, Nagy A, Lobe CG, Whitsett JA (2002) Early restriction of peripheral and proximal cell lineages during formation of the lung. *Proc Natl Acad Sci USA* 99(16):10482–10487.
6. Miller LA, et al. (2004) Role of Sonic hedgehog in patterning of tracheal-bronchial cartilage and the peripheral lung. *Dev Dyn* 231(1):57–71.
7. Rock JR, Futtner CR, Harfe BD (2008) The transmembrane protein TMEM16A is required for normal development of the murine trachea. *Dev Biol* 321(1):141–149.
8. Geng Y, et al. (2011) Follistatin-like 1 (Fstl1) is a bone morphogenetic protein (BMP) 4 signaling antagonist in controlling mouse lung development. *Proc Natl Acad Sci USA* 108(17):7058–7063.
9. Foster JW, et al. (1994) Campomelic dysplasia and autosomal sex reversal caused by mutations in an SRY-related gene. *Nature* 372(6506):525–530.
10. Kwok C, et al. (1995) Mutations in SOX9, the gene responsible for Campomelic dysplasia and autosomal sex reversal. *Am J Hum Genet* 57(5):1028–1036.
11. Bi W, Deng JM, Zhang Z, Behringer RR, de Crombrugghe B (1999) Sox9 is required for cartilage formation. *Nat Genet* 22(1):85–89.
12. Ng LJ, et al. (1997) SOX9 binds DNA, activates transcription, and coexpresses with type II collagen during chondrogenesis in the mouse. *Dev Biol* 183(1):108–121.
13. Zhao Q, Eberspaecher H, Lefebvre V, De Crombrugghe B (1997) Parallel expression of Sox9 and Col2a1 in cells undergoing chondrogenesis. *Dev Dyn* 209(4):377–386.
14. Akiyama H, Chaboissier MC, Martin JF, Schedl A, de Crombrugghe B (2002) The transcription factor Sox9 has essential roles in successive steps of the chondrocyte differentiation pathway and is required for expression of Sox5 and Sox6. *Genes Dev* 16(21):2813–2828.
15. Wagner T, et al. (1994) Autosomal sex reversal and campomelic dysplasia are caused by mutations in and around the SRY-related gene SOX9. *Cell* 79(6):1111–1120.
16. Bi W, et al. (2001) Haploinsufficiency of Sox9 results in defective cartilage primordia and premature skeletal mineralization. *Proc Natl Acad Sci USA* 98(12):6698–6703.
17. Akiyama H, et al. (2004) Interactions between Sox9 and beta-catenin control chondrocyte differentiation. *Genes Dev* 18(9):1072–1087.
18. Shao Y, Alicknavitch M, Farach-Carson MC (2005) Expression of voltage sensitive calcium channel (VSCC) L-type Cav1.2 (alpha1C) and T-type Cav3.2 (alpha1H) subunits during mouse bone development. *Dev Dyn* 234(1):54–62.
19. Mancilla EE, et al. (2007) L-type calcium channels in growth plate chondrocytes participate in endochondral ossification. *J Cell Biochem* 101(2):389–398.
20. Matta C, et al. (2008) Cytosolic free Ca2+ concentration exhibits a characteristic temporal pattern during in vitro cartilage differentiation: A possible regulatory role of calcineurin in Ca-signalling of chondrogenic cells. *Cell Calcium* 44(3):310–323.
21. Bergh JJ, Shao Y, Puente E, Duncan RL, Farach-Carson MC (2006) Osteoblast Ca(2+) permeability and voltage-sensitive Ca(2+) channel expression is temporally regulated by 1,25-dihydroxyvitamin D(3). *Am J Physiol Cell Physiol* 290(3):C822–C831.
22. Senatore A, Spafford JD (2012) Gene transcription and splicing of T-type channels are evolutionarily-conserved strategies for regulating channel expression and gating. *PLoS ONE* 7(6):e37409.
23. Catterall WA (2011) Voltage-gated calcium channels. *Cold Spring Harb Perspect Biol* 3(8):a003947.
24. Perez-Reyes E, Lory P (2006) Molecular biology of T-type calcium channels. *CNS Neurol Disord Drug Targets* 5(6):605–609.
25. Chen Y, et al. (2003) Association between genetic variation of CACNA1H and childhood absence epilepsy. *Ann Neurol* 54(2):239–243.
26. Zhong X, Liu JR, Kyle JW, Hanck DA, Agnew WS (2006) A profile of alternative RNA splicing and transcript variation of CACNA1H, a human T-channel gene candidate for idiopathic generalized epilepsies. *Hum Mol Genet* 15(9):1497–1512.
27. Heron SE, et al. (2007) Extended spectrum of idiopathic generalized epilepsies associated with CACNA1H functional variants. *Ann Neurol* 62(6):560–568.
28. Chen CC, et al. (2003) Abnormal coronary function in mice deficient in alpha1H T-type Ca2+ channels. *Science* 302(5649):1416–1418.
29. Chiang CS, et al. (2009) The Ca(v)3.2 T-type Ca(2+) channel is required for pressure overload-induced cardiac hypertrophy in mice. *Circ Res* 104(4):522–530.
30. Shin HS, Cheong EJ, Choi S, Lee J, Na HS (2008) T-type Ca2+ channels as therapeutic targets in the nervous system. *Curr Opin Pharmacol* 8(1):33–41.
31. Chen WK, et al. (2010) Ca(v)3.2 T-type Ca2+ channel-dependent activation of ERK in paraventricular thalamus modulates acid-induced chronic muscle pain. *J Neurosci* 30(31):10360–10368.
32. Wang R, Lewin GR (2011) The Cav3.2 T-type calcium channel regulates temporal coding in mouse mechanoreceptors. *J Physiol* 589(Pt 9):2229–2243.
33. Chen CC, et al. (2012) Retrieval of context-associated memory is dependent on the Ca(v)3.2 T-type calcium channel. *PLoS ONE* 7(1):e29384.
34. Park J, et al. (2010) Regulation of Sox9 by Sonic Hedgehog (Shh) is essential for patterning and formation of tracheal cartilage. *Dev Dyn* 239(2):514–526.
35. Que J, et al. (2007) Multiple dose-dependent roles for Sox2 in the patterning and differentiation of anterior foregut endoderm. *Development* 134(13):2521–2531.
36. Atsumi T, Miwa Y, Kimata K, Ikawa Y (1990) A chondrogenic cell line derived from a differentiating culture of AT805 teratocarcinoma cells. *Cell Differ Dev* 30(2):109–116.
37. Huang L, et al. (2004) NNC 55-0396 [(1S,2S)-2-(2-(N-[(3-benzimidazol-2-yl)propyl]-N-methylamino)ethyl)-6-fluoro-1,2,3,4-tetrahydro-1-isopropyl-2-naphtyl cyclopropanecarboxylate dihydrochloride]: A new selective inhibitor of T-type calcium channels. *J Pharmacol Exp Ther* 309(1):193–199.
38. Tomita M, Reinhold MI, Molkentin JD, Naski MC (2002) Calcineurin and NFAT4 induce chondrogenesis. *J Biol Chem* 277(44):42214–42218.
39. Huang CH, Chen YC, Chen CC (2013) Physical interaction between calcineurin and Cav3.2 T-type Ca2+ channel modulates their functions. *FEBS Lett* 587(12):1723–1730.
40. Wilkins BJ, et al. (2004) Calcineurin/NFAT coupling participates in pathological, but not physiological, cardiac hypertrophy. *Circ Res* 94(1):110–118.
41. Martin JF, Bradley A, Olson EN (1995) The paired-like homeo box gene MHox is required for early events of skeletogenesis in multiple lineages. *Genes Dev* 9(10):1237–1249.
42. Akiyama H, et al. (2005) Osteo-chondroprogenitor cells are derived from Sox9 expressing precursors. *Proc Natl Acad Sci USA* 102(41):14665–14670.
43. Sekiya I, et al. (2000) SOX9 enhances aggrecan gene promoter/enhancer activity and is up-regulated by retinoic acid in a cartilage-derived cell line, TC6. *J Biol Chem* 275(15):10738–10744.
44. Lefebvre V, Huang W, Harley VR, Goodfellow PN, de Crombrugghe B (1997) SOX9 is a potent activator of the chondrocyte-specific enhancer of the pro alpha1(II) collagen gene. *Mol Cell Biol* 17(4):2336–2346.
45. Akiyama H (2008) Control of chondrogenesis by the transcription factor Sox9. *Mod Rheumatol* 18(3):213–219.
46. Morishita M, et al. (2001) A 30-base-pair element in the first intron of SOX9 acts as an enhancer in ATDC5. *Biochem Biophys Res Commun* 288(2):347–355.
47. Xie X, et al. (2007) Validation of high throughput screening assays against three subtypes of Ca(v)3 T-type channels using molecular and pharmacologic approaches. *Assay Drug Dev Technol* 5(2):191–203.
48. Messeguer X, et al. (2002) PROMO: Detection of known transcription regulatory elements using species-tailored searches. *Bioinformatics* 18(2):333–334.
49. Zuscik MJ, Hilton MJ, Zhang X, Chen D, O'Keefe RJ (2008) Regulation of chondrogenesis and chondrocyte differentiation by stress. *J Clin Invest* 118(2):429–438.
50. Lory P, Bidaud I, Chemin J (2006) T-type calcium channels in differentiation and proliferation. *Cell Calcium* 40(2):135–146.
51. Li Y, et al. (2009) A role of functional T-type Ca2+ channel in hepatocellular carcinoma cell proliferation. *Oncol Rep* 22(5):1229–1235.
52. Thompson WR, et al. (2011) Association of the α(2)δ(1) subunit with Ca(v)3.2 enhances membrane expression and regulates mechanically induced ATP release in MLO-Y4 osteocytes. *J Bone Miner Res* 26(9):2125–2139.
53. Choi J, et al. (2005) T-type calcium channel trigger p21ras signaling pathway to ERK in Cav3.1-expressed HEK293 cells. *Brain Res* 1054(1):22–29.
54. Nakayama H, et al. (2009) alpha1G-dependent T-type Ca2+ current antagonizes cardiac hypertrophy through a NOS3-dependent mechanism in mice. *J Clin Invest* 119(12):3787–3796.

55. Yao J, et al. (2006) Molecular basis for the modulation of native T-type Ca2+ channels in vivo by Ca2+/calmodulin-dependent protein kinase II. *J Clin Invest* 116(9): 2403–2412.
56. Rodman DM, et al. (2005) Low-voltage-activated (T-type) calcium channels control proliferation of human pulmonary artery myocytes. *Circ Res* 96(8):864–872.
57. Pluteanu F, Cribbs LL (2011) Regulation and function of Cav3.1 T-type calcium channels in IGF-I-stimulated pulmonary artery smooth muscle cells. *Am J Physiol Cell Physiol* 300(3):C517–C525.
58. Tzeng BH, et al. (2012) The Cav3.1 T-type calcium channel is required for neointimal formation in response to vascular injury in mice. *Cardiovasc Res* 96(3):533–542.
59. Lu F, et al. (2008) T-type Ca2+ channel expression in human esophageal carcinomas: A functional role in proliferation. *Cell Calcium* 43(1):49–58.
60. Toyota M, Ho C, Ohe-Toyota M, Baylin SB, Issa JP (1999) Inactivation of CACNA1G, a T-type calcium channel gene, by aberrant methylation of its 5′ CpG island in human tumors. *Cancer Res* 59(18):4535–4541.
61. Oguri A, et al. (2010) Involvement of CaV3.1 T-type calcium channels in cell proliferation in mouse preadipocytes. *Am J Physiol Cell Physiol* 298(6):C1414–C1423.
62. Bijlenga P, et al. (2000) T-type alpha 1H Ca2+ channels are involved in Ca2+ signaling during terminal differentiation (fusion) of human myoblasts. *Proc Natl Acad Sci USA* 97(13):7627–7632.
63. Chemin J, Nargeot J, Lory P (2002) Neuronal T-type alpha 1H calcium channels induce neuritogenesis and expression of high-voltage-activated calcium channels in the NG108-15 cell line. *J Neurosci* 22(16):6856–6862.
64. Kushmerick C, Romano-Silva MA, Gomez MV, Prado MA (2001) Changes in Ca(2+) channel expression upon differentiation of SN56 cholinergic cells. *Brain Res* 916(1-2): 199–210.
65. Mariot P, Vanoverberghe K, Lalevee N, Rossier MF, Prevarskaya N (2002) Overexpression of an alpha 1H (Cav3.2) T-type calcium channel during neuroendocrine differentiation of human prostate cancer cells. *J Biol Chem* 277(13):10824–10833.
66. Senatore A, Zhorov BS, Spafford JD (2012) Cav3 T-type calcium channels. *Wiley Interdiscip Rev Membr Transp Signal* 1(4):467–491.
67. Ramage L, Martel MA, Hardingham GE, Salter DM (2008) NMDA receptor expression and activity in osteoarthritic human articular chondrocytes. *Osteoarthritis Cartilage* 16(12):1576–1584.
68. Salter DM, Wright MO, Millward-Sadler SJ (2004) NMDA receptor expression and roles in human articular chondrocyte mechanotransduction. *Biorheology* 41(3-4):273–281.
69. Fodor J, et al. (2013) Store-operated calcium entry and calcium influx via voltage-operated calcium channels regulate intracellular calcium oscillations in chondrogenic cells. *Cell Calcium* 54(1):1–16.
70. Jahr H, van Driel M, van Osch GJ, Weinans H, van Leeuwen JP (2005) Identification of acid-sensing ion channels in bone. *Biochem Biophys Res Commun* 337(1):349–354.
71. Gavenis K, et al. (2009) Expression of ion channels of the TRP family in articular chondrocytes from osteoarthritic patients: Changes between native and in vitro propagated chondrocytes. *Mol Cell Biochem* 321(1-2):135–143.
72. O'Conor CJ, Leddy HA, Benefield HC, Liedtke WB, Guilak F (2014) TRPV4-mediated mechanotransduction regulates the metabolic response of chondrocytes to dynamic loading. *Proc Natl Acad Sci USA* 111(4):1316–1321.
73. Clark AL, Votta BJ, Kumar S, Liedtke W, Guilak F (2010) Chondroprotective role of the osmotically sensitive ion channel transient receptor potential vanilloid 4: Age- and sex-dependent progression of osteoarthritis in Trpv4-deficient mice. *Arthritis Rheum* 62(10):2973–2983.
74. Liu Y, Li H, Tanaka K, Tsumaki N, Yamada Y (2000) Identification of an enhancer sequence within the first intron required for cartilage-specific transcription of the alpha2(XI) collagen gene. *J Biol Chem* 275(17):12712–12718.
75. Piera-Velazquez S, et al. (2007) Regulation of the human SOX9 promoter by Sp1 and CREB. *Exp Cell Res* 313(6):1069–1079.
76. Ushita M, et al. (2009) Transcriptional induction of SOX9 by NF-kappaB family member RelA in chondrogenic cells. *Osteoarthritis Cartilage* 17(8):1065–1075.
77. Colter DC, et al. (2005) Regulation of the human Sox9 promoter by the CCAAT-binding factor. *Matrix Biol* 24(3):185–197.
78. Bradley EW, Drissi MH (2010) WNT5A regulates chondrocyte differentiation through differential use of the CaN/NFAT and IKK/NF-kappaB pathways. *Mol Endocrinol* 24(8): 1581–1593.
79. de Jong EM, et al. (2010) 5q11.2 deletion in a patient with tracheal agenesis. *Eur J Hum Genet* 18(11):1265–1268.
80. Hockstein NG, et al. (2004) Tracheal anomalies in Pfeiffer syndrome. *Arch Otolaryngol Head Neck Surg* 130(11):1298–1302.
81. Furtado LV, et al. (2011) Unilateral sclerocornea and tracheal stenosis: Unusual findings in a patient with Goldenhar anomaly. *Fetal Pediatr Pathol* 30(6):397–404.
82. Li BC, et al. (2013) Clinical report: Two patients with atelosteogenesis type I caused by missense mutations affecting the same FLNB residue. *Am J Med Genet A* 161A(3): 619–625.
83. Bell SM, et al. (2008) R-spondin 2 is required for normal laryngeal-tracheal, lung and limb morphogenesis. *Development* 135(6):1049–1058.
84. Li C, Xiao J, Hormi K, Borok Z, Minoo P (2002) Wnt5a participates in distal lung morphogenesis. *Dev Biol* 248(1):68–81.
85. Geng Y, et al. (2011) Follistatin-like 1 (Fstl1) is a bone morphogenetic protein (BMP) 4 signaling antagonist in controlling mouse lung development. *Proc Natl Acad Sci USA* 108(17):7058–7063.
86. Li Y, Gordon J, Manley NR, Litingtung Y, Chiang C (2008) Bmp4 is required for tracheal formation: A novel mouse model for tracheal agenesis. *Dev Biol* 322(1):145–155.
87. Tiozzo C, et al. (2009) Fibroblast growth factor 10 plays a causative role in the tracheal cartilage defects in a mouse model of Apert syndrome. *Pediatr Res* 66(4):386–390.
88. Sala FG, et al. (2011) FGF10 controls the patterning of the tracheal cartilage rings via Shh. *Development* 138(2):273–282.
89. Lerman G, et al. (2011) MiRNA expression in psoriatic skin: Reciprocal regulation of hsa-miR-99a and IGF-1R. *PLoS ONE* 6(6):e20916.
90. Bonvin E, et al. (2008) Congenital tracheal malformation in cystic fibrosis transmembrane conductance regulator-deficient mice. *J Physiol* 586(13):3231–3243.
91. Hsu SC, Chang YT, Chen CC (2013) Early growth response 1 is an early signal inducing Cav3.2 T-type calcium channels during cardiac hypertrophy. *Cardiovasc Res* 100(2): 222–230.
92. Lee TI, Johnstone SE, Young RA (2006) Chromatin immunoprecipitation and microarray-based analysis of protein location. *Nat Protoc* 1(2):729–748.